



# INFLUENCE OF ACTIVE GAS CONTENT AND DISPERSE FILLER CONTINUITY ON THE PROCESS OF BEAD FORMATION IN MICROPLASMA POWDER SURFACING OF NICKEL SUPERALLOYS

K.A. YUSHCHENKO and A.V. YAROVITSYN

E.O. Paton Electric Welding Institute, NASU  
11 Bozhenko Str., 03680, Kiev, Ukraine. E-mail: office@paton.kiev.ua

Features of deposited metal formation in microplasma powder surfacing of nickel superalloys, depending on presence of active gases in the filler powder, are considered. Conditions of sound formation of deposited metal and requirements to filler powders were established, proceeding from oxygen and nitrogen content. An interrelation between presence of micropores in deposited metal and their presence inside disperse powder particles is shown. A probable mechanism of microporosity formation, influence of technological parameters of the process on micropore quantity and size in deposited metal is described. 25 Ref., 2 Tables, 10 Figures.

**Keywords:** *microplasma powder surfacing, nickel superalloys, deposited metal, filler powder, oxygen and nitrogen, microporosity of powder and deposited metal*

It is known that presence of defects in welded joints, in particular, deviations from the specified shape and continuity of deposited metal, leads to considerable lowering of item service properties [1].

The main  $\gamma'$ -forming elements of high-temperature nickel alloys — aluminium and titanium, chromium, as well as other refractory alloying elements — because of their high affinity to oxygen are the cause for formation of refractory oxides in fusion welding [2–5], in particular, inclusions in deposited metal and lacks-of-fusion. Their presence in the weld pool necessitates an essential increase of welding current, in order to ensure an acceptable spreadability of metal being deposited [4, 5]. In view of limited solubility of nickel alloys with  $\gamma'$ -phase content of more than 45 vol.%, increase of specific heat input increases the probability of hot cracking in welding and of crack initiation during subsequent heat treatment [2, 5, 6]. Therefore, ensuring sound formation of deposited metal for such materials is closely related to technological strength of welded joint and, alongside the optimum structure, it is a most important component of welded joint quality and operating reliability.

Process of microplasma powder surfacing is applied in repair of sealing, antivibration elements of aircraft gas turbine engine blades [7,

8]. For this process filler disperse powders of nickel alloys with different content of  $\gamma'$ -phase are batch produced. Penetration of relatively small quantities of active gases into deposited metal of nickel superalloys [9] can cause deviations from its sound formation. Proceeding from experience of surfacing and operation of reconditioned blades, quality of disperse filler is important, which, in particular, is determined by oxygen and nitrogen content.

Negative influence of micropores in disperse particles on item performance is known in powder metallurgy. Mechanism of their formation during melt dispersion by inert gas is described in [2, 10, 11]. It runs in four stages: introduction of portions of energy carrier gas into the melt jet flowing out of the atomizer; decomposition of gas portions into bubbles in molten metal jet; jet decomposition into fragments, part of which carries gas bubbles; cooling and solidification of metal drops with gas bubbles or without them. Owing to limited heat input into the item and time of weld pool metal staying in the molten state, continuity of filler powder particles can also affect the process of deposited bead formation in microplasma surfacing.

The objective of this work is more precise definition of ranges of oxygen and nitrogen content in disperse filler material, as well as studying the causes and regularities of microporosity formation in deposited metal of nickel superalloys.

Objects of research were deposited metal and filler powders of nickel superalloys with  $\gamma'$ -phase content of more than 45 vol.%. Vacuum extrac-



tion method was used for quantitative evaluation of active gases in the metal [9, 12, 13]. Active gas content in the cast, deposited metal and filler powder was determined in the LECO systems RO316 (oxygen) and TN114 (nitrogen).

Filler powders of nickel and cobalt alloys with particles size of 63–160  $\mu\text{m}$  were used in surfacing. The following parameters were varied for metallographic investigation of the deposited metal:

- welding current of 10–65 A;
- diameter of plasmatron focusing nozzle  $d_f = 5.5$  and 3.0 mm, which determined 4.8–20  $\text{cm}^{-2}$  concentration of powder feeding into the weld pool by the procedure of [14];
- kind of powder feed (continuous in the quantity  $G = 5$  g/min or portioned feed with microportion weight  $M_0 = 0.02$ –0.14 g, and their feeding periodicity  $t_p = 0.5$ –2.5 s).

Blanks of deposited metal sample sections and filler powder samples were pressed into plastic holders of 30 mm diameter in the Struers Labo-Press-3. Metallographic analysis of longitudinal section of deposited metal bead (sample length of 15 to 22 mm) was performed in optical microscope Neophot 32. Analysis of quantitative content of micropores in filler powders was conducted by photos taken in Jenavert optical microscope with digital camera Micam TCA-5.0. This allowed detection of micropores greater than

5  $\mu\text{m}$  in the deposited metal and filler powders, and evaluation of their size with the accuracy of  $\pm 2.5$   $\mu\text{m}$ . At calculation of micropore area it was assumed that its cross-sectional shape is a circumference.

In case of micropore detection their following quantitative characteristics were determined: for deposited metal – total micropore area  $F_{PD}$  over an area of 50  $\text{mm}^2$ ; relative micropore area  $\Pi_{PD} = 0.02F_{PD}$ ; for photos with cross-section of filler powder particles – total particle number  $N$ ; number of particles with micropores  $N_{MPP}$ ; relative number of particles with micropores  $\Pi_{MPP} = N_{MPP}/N$ ; total micropore area  $F_{MPP}$ ; conditional micropore area per one powder particles  $F_{MPP}/N$ . Analysis of disperse filler particles was conducted in six nonintersecting fields of vision for each, stage size was approximately 2  $\text{mm}^2$ ; total particle quantity was equal to about 1500 pcs. Microstructure of filler powders and individual particles was examined further in electron microscope in back-scattered electrons.

Evaluation of picnometric density of powder and its porosity was performed by the procedure of [15]. Weight of powder sample was  $15 \pm 0.03$  g. Before pouring into the densimeter, the powder was dried in air at 150  $^{\circ}\text{C}$  for 0.5 h. Ethyl alcohol was used as picnometric liquid. Densimeter mass at successive weighing was determined

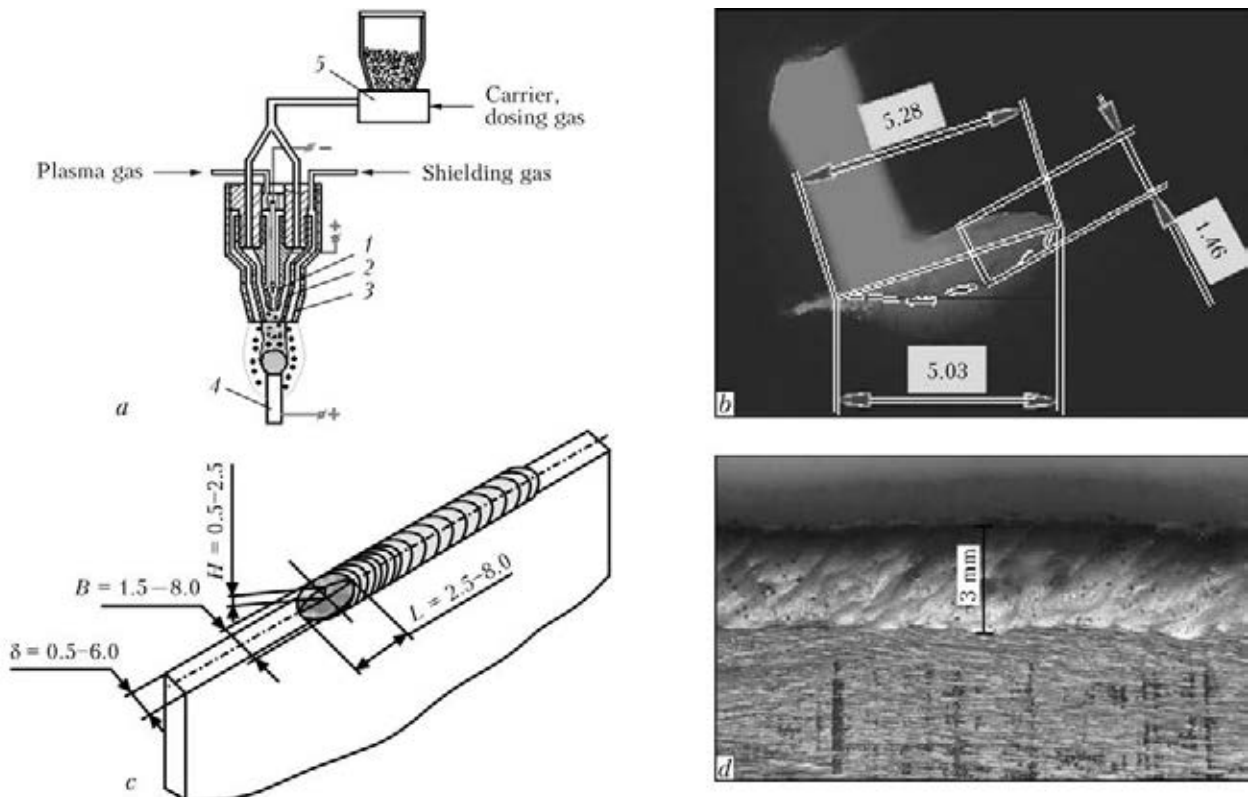


**Figure 1.** Schematic of the process of microplasma powder surfacing (*a*: 1 – plasma nozzle; 2 – focusing orifice; 3 – protective cone; 4 – item; 5 – powder feeder), weld pool appearance (*b*), its typical dimensions (*c*), and deposited bead appearance (*d*)

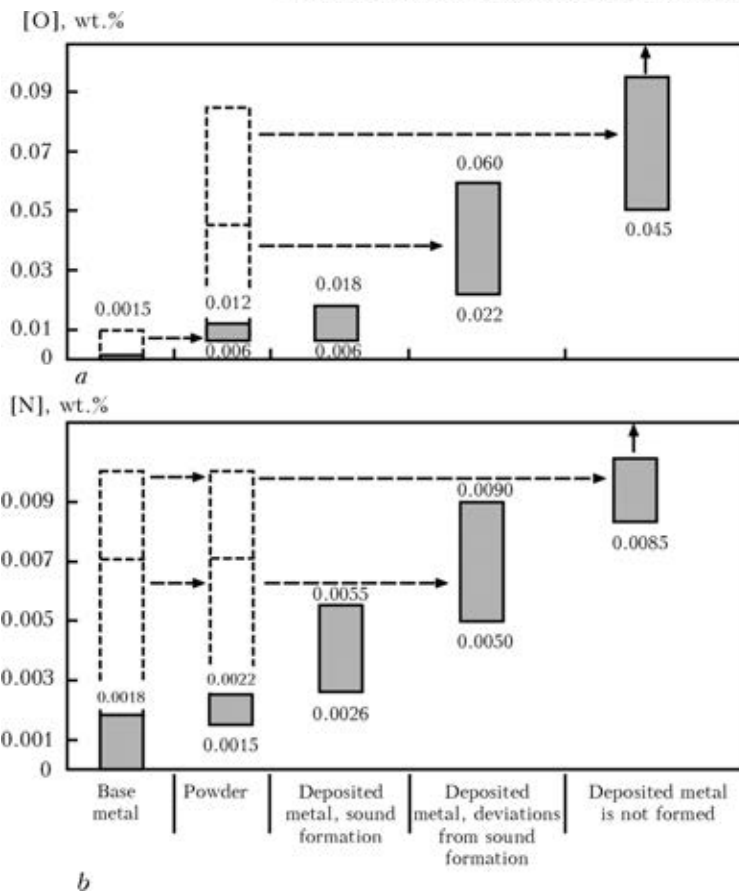


**Figure 2.** Content of oxygen (a) and nitrogen (b) after superalloy going through cast billet–disperse powder–deposited metal technological stages (*dashed line* – possible deviations from recommended ranges of active gas content in the metal)

in analytical scales VLP-200 of the 2nd accuracy class to GOST 19491–74. Measurements were performed by direct weighing with the accuracy of  $\pm 2.5$  mg. Porosity, determined by the procedure of hydrostatic weighing, was calculated as

$$\Pi_{wt} = 100(1 - \rho_p / \rho) (\%),$$

where  $\rho_p$  is the pycnometric density of powder;  $\rho$  is the alloy density.

Results of metallographic analysis and hydrostatic weighing after statistical treatment were correlated with process parameters and features of microplasma powder surfacing.

Schematic and features of the process of microplasma powder surfacing are given in Figure 1. As a rule, as current of up to 35 A the weld pool has the shape of an ellipsoid. Depending on the value of specific heat input, the volume of its liquid metal is from 2 up to 125 mm<sup>3</sup>. Duration of it staying in the molten state is from 2 to 20 s.

Change of oxygen and nitrogen content in the nickel alloy with  $\gamma'$ -phase quantity greater than 45 vol.% has been analyzed after the following metallurgical processing stages: cast billet–dis-

persed powder–deposited metal allowing for the features of its formation (Figures 2 and 3). Earlier published in our work [9] data were complemented, generalized and are presented in Figure 2 in the form of a range of these gases content. It is shown that sound formation of deposited metal is achieved at its content of oxygen of not more than 0.018 % and of nitrogen of not more than 0.0055 wt.%. Visual observations showed that the deposited metal readily spreads and wets the base metal; oxide film on weld pool surface is absent.

Deposited metal formation is impaired, if the content of oxygen and nitrogen in the deposited metal rises above 0.022 and 0.005 wt.%, respectively (see Figures 2 and 3). Then, the following features are observed in surfacing:

- dense oxide film forms on greater part of weld pool surface, which can remain on bead surface after deposition;
- pool width is much greater than that of narrow substrate\* (more than 1.5–2.0 mm to one side), that makes subsequent bead machining more complicated;

\*Surface, the width of which is not greater than that of weld pool [16].

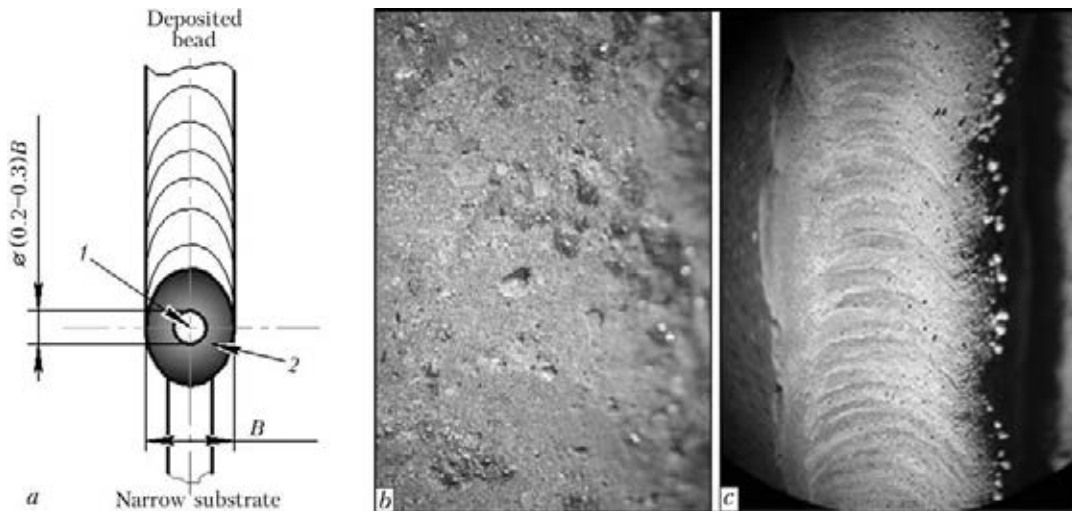


**Figure 3.** Features of formation of deposited nickel superalloy with more than 45 vol.% of  $\gamma'$ -phase at increased content of oxygen and nitrogen in it: *a* – weld pool (1 – free section of weld pool surface; 2 – weld pool surface periphery covered by oxide film); *b* – oxide film after bead solidification ( $\times 25$ ); *c* – bead appearance

- lacks-of-fusion, oxide inclusions and undercuts periodically form in the deposited metal and on its interface with base metal.

If oxygen and nitrogen content in the deposited metal is more than 0.045–0.060 and 0.0085–0.0090 wt.%, respectively, then continuous formation of deposited metal is disturbed because of presence of dense oxide films (see Figure 2).

The above-described deviations from sound formation of deposited nickel superalloys are also manifested to varying degrees, if oxygen and nitrogen content in the disperse filler exceeds 0.0120 and 0.0022 wt.%, respectively (see Figures 2 and 3). In its turn, quantity of active gases in the powder depends on their content in the initial cast billet [17–20]; method to produce powder [16]; level of humidity of powdered materials [9, 16]; repetition factor of powder use [9, 16].

It is known that oxygen and nitrogen, alongside other elements, are impurities in cast nickel superalloys. Their content in modern alloys after vacuum-induction melting is limited to 0.0015 wt.% [17, 18]. Increase of the content of oxygen to 0.0017–0.0032 and of nitrogen to 0.0015–0.01 wt.% in initial castings can be due to addition of casting production wastes to charge materials [17–20]. Powder remains after reuse [9, 14, 21], wastes from powder manufacture [10, 11] (disperse material outside 40 to 250  $\mu\text{m}$  fraction) can, probably, also be used in the initial billet for powder dispersion and can essentially increase oxygen content in it (tentatively up to 0.012 wt.%). In this case, increased content of active gases in disperse powder can in itself cause unsound formation of deposited bead.

Powder dispersion method can have an essential influence on oxygen and nitrogen content in the disperse filler. Surfacing powders with differ-

ent dispersion of liquid metal jet, namely by water, air or nitrogen, argon under pressure, and with centrifugal dispersion are batch produced. Oxygen and nitrogen content in them is determined by the medium dispersing the melt, and can be quite high: 0.06–0.12 and 0.061–0.141 wt.%, respectively [16]. For instance, evaluation of the content of active gases in filler powders of nickel alloy IN625 of a number of manufacturers showed that in some cases it may reach 0.04–0.05 wt.% O and 0.007–0.009 wt.% N.

In view of the high affinity to oxygen of the main alloying elements in superalloys, the technology of disperse filler manufacturing should provide guaranteed protection from the impact of active gases on the melt. Method of ingot dispersion by argon with powder cooling in inert medium the most completely meets these requirements [10, 11]. At gas content limited to 0.002 wt.% in the initial billet, it allows producing filler powder from nickel superalloys with oxygen content of up to 0.012 and nitrogen content of up to 0.0025 wt.%.

In microplasma powder surfacing, part of the filler moves around the microplasma arc periphery, does not penetrate into the weld pool, and can be reused [9, 14, 21]. During investigation of such powder morphology by optical microscopy methods (Figure 4, *a*) it is established that at its multiple application it accumulates particles with oxidized surface (up to 50–60 % of the total quantity). Electron microscopy analysis of these particles showed presence of an oxide film of 3 to 4  $\mu\text{m}$  thickness on their surface (Figure 4, *c–d*). Application of such powder only slightly increases oxygen and nitrogen content in the deposited metal – not more than 0.003–

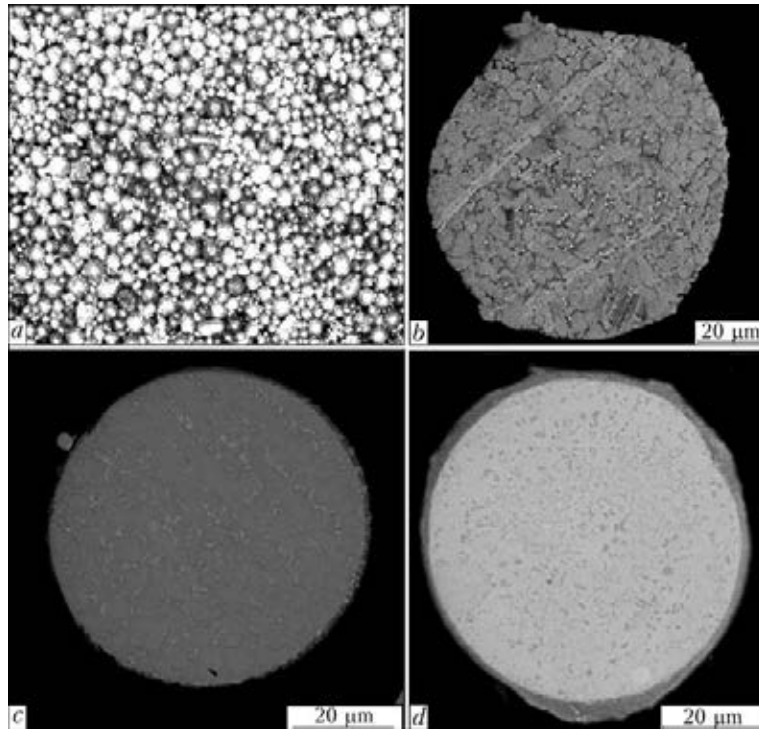


**Figure 4.** Morphology and microstructure of transverse section of particles of nickel superalloy powder: *a* – powder remains after reusing it several times (darker surface colour – particles oxidized in microplasma arc) ( $\times 50$ ); *b* – particle of new powder from JS6U-VI alloy ( $\times 650$ ); *c* – particle of JS32-VI alloy powder oxidized in microplasma arc ( $\times 1000$ ); *d* – particle of JS32-VI alloy powder oxidized and remelted in microplasma arc ( $\times 1000$ )

0.0015 wt.%, respectively [9], that is admissible at ensuring sound bead formation, oxygen and nitrogen content in the deposited metal not exceeding 0.018 and 0.0055 wt.%, respectively.

At metallographic analysis micropores of 5–75  $\mu\text{m}$  size (predominantly 20–40  $\mu\text{m}$ ) in the quantity of 20–30 pcs over an area of approximately 4  $\text{mm}^2$  are periodically revealed in the metal of nickel alloys with  $\gamma'$ -phase content of 15 to 62 vol.% produced by microplasma powder surfacing. Both their uniform distribution and local elongated clusters of micropores, irrespective of the distance from the fusion line, are observed in the deposited metal (Figure 5).

Micropore presence in the deposited metal is not influenced by the kind of shielding gas (argon, argon-hydrogen mixture [7]) or parameters

of the mode of powder pre-drying at 300  $^{\circ}\text{C}$ . Investigations of longitudinal sections of beads, deposited predominantly at effective heating power of 200–500 W, showed that over deposited metal area of 50  $\text{mm}^2$  total area of micropores  $F_{\text{PD}}$  is in the range of 1000–70,000  $\mu\text{m}^2$ , and their relative area  $\Pi_{\text{PD}}$  is equal to 0.002–0.140 vol.%.

Appearance of micropores of 5–75  $\mu\text{m}$  size in the deposited metal is associated with presence of predominantly closed micropores of similar size in the filler powder (Figure 6). Electron microscopy analysis of cross-sections of powder particles with inner discontinuities demonstrated absence of oxide films on micropore outer boundary (Figure 6, *c-f*). This is indicative of sufficiently high level of protection from the air medium in melt dispersion and is not contradictory

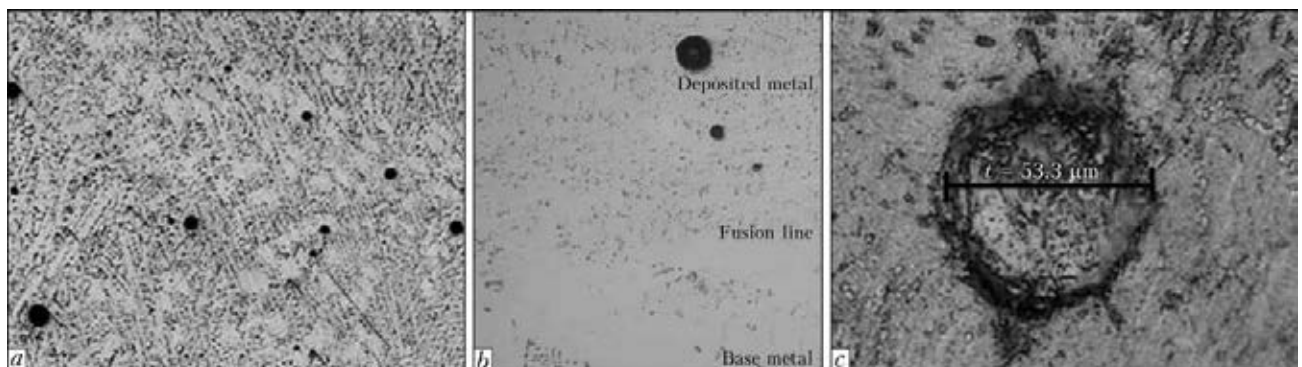


**Figure 5.** Microstructure of deposited metal with micropores (*a* –  $\times 50$ ; *b* –  $\times 100$ ), and isolated micropore (*c*) in deposited metal of JS32 alloy (*a*, *c* – chemical; *b* – ion etching)

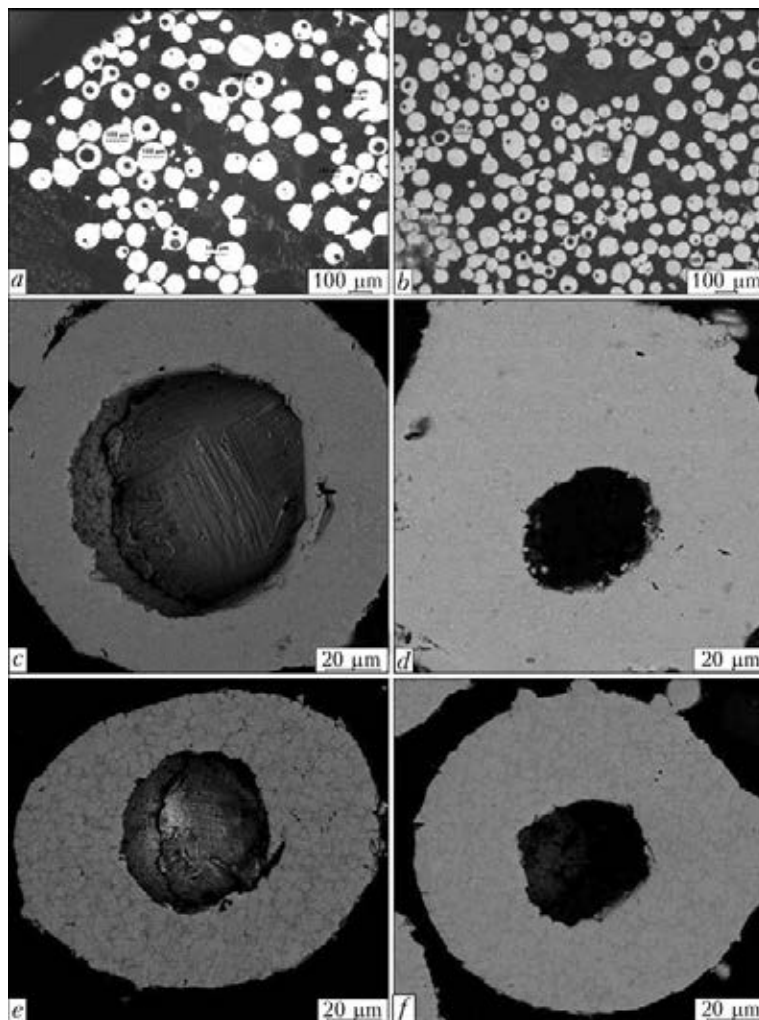


**Figure 6.** Microstructure of particles of nickel superalloy powder with micropores: *a-d* – powder from JS32-VI alloy; optical (*a, b*) and electron microscopy (*c, d*) data; *e* – powder from JS26-VI alloy; *f* – powder from JS6U-VI alloy

to described in [2, 10, 11] mechanism of micropore formation.

Metallographic analysis of samples taken from ten batches of filler powder from nickel and cobalt alloys, confirmed the fact of presence of micropores in them, irrespective of alloy grade or powder manufacturer. It is established that the content of inner micropores in the disperse filler rises significantly with increase of quantity of  $\gamma'$ -phase above 45–50 vol.% in the nickel alloy, and specific fraction of particles of more than 100–125  $\mu\text{m}$  size in granulometric composition of used powder fraction. Quantitative characteristics of microporosity for batches of filler powder from JS32-VI alloy are given in Table 1.

Figures 7–9 show the change of quantitative characteristics of microporosity in the deposited metal depending on surfacing process technological parameters and quantitative characteristics of filler powder microporosity. It is established that in microplasma surfacing with  $I = \text{const}$  and powder feed  $G = 5 \text{ g/min}$ , they depend on:

- quantitative content and size of micropores in the initial filler, decreasing to  $\Pi_{\text{PD}} = 0.01\text{--}0.026 \text{ vol.}\%$  at their lowering ( $\Pi_{\text{MPP}} = 2.13\text{--}4.51 \%$  and  $F_{\text{MPP}}/N = 2.13\text{--}6.56 \mu\text{m}^2/\text{pcs}$ );

- welding current value, decreasing to  $\Pi_{\text{PD}} = 0.03\text{--}0.06 \text{ vol.}\%$  at 45–65 A;

- concentration of powder feeding, weight of added powder microportions  $M_0 = 0.02\text{--}0.13 \text{ g}$ , their feeding periodicity  $t_p = 0.5\text{--}2.5 \text{ s}$ .

Minimum content of micropores in the deposited JS32 metal ( $\Pi_{\text{PD}} = 0.02\text{--}0.03 \text{ vol.}\%$ ) is observed at reduction of weight of filler powder microportion to 0.02 g (see Figure 9).

To limit the quantity and size of micropores in the deposited metal at application of disperse filler containing a considerable quantity of micropores (for instance,  $\Pi_{\text{PD}} = 13.46 \%$  and  $F_{\text{MPP}}/N = 48.02 \mu\text{m}^2/\text{pcs}$ ), powder should be fed in small microportions ( $M_0 \approx 0.02 \text{ g}$ ) with not more than 2.5 s periodicity. In this case containing the weld pool on a narrow substrate requires more precise metering of heat input into the item, in order to reduce base metal penetra-



**Table 1.** Microporosity characteristics of filler powder from JS32-VI alloy (by metallographic analysis data)

Fraction, $\mu\text{m}$ (GOST 6613-86) Powder microporosity parameters	I batch	II batch		III batch	
	$\Pi_{\text{MPPf}}, \%$	$N_f/N, \%$	$\Pi_{\text{MPPf}}, \%$	$N_f/N, \%$	$\Pi_{\text{MPPf}}, \%$
-63	0.19	31.66	0.73	29.74	0.65
63-80	-	19.92	3.71	32.09	10.66
80-100	-	19.73	5.02	28.94	16.07
100-125	-	19.19	8.44	8.02	37.03
125-160	-	8.51	52.17	1.96	30.10
$\Pi_{\text{MPP}}, \%$	0.19	-	8.68	-	13.46
$F_{\text{MPP}}/N, \mu\text{m}^2/\text{pcs}$	7.57	-	36.37	-	48.02

Note.  $N_f/N$  – relative quantity of powder particles in the fraction;  $\Pi_{\text{MPPf}}$  – relative quantity of particles with micropores in the fraction.

tion depth. Such a principle of mode selection is essentially different from plasma-powder surfacing [16] or welding with additional disperse filler [22], where base metal penetration is limited by addition of considerable amounts of disperse filler to the weld pool.

Experimental data (see Figures 7-9) allow assuming that micropore formation in the deposited metal differs from the generally known mechanism of porosity formation in welds [1]. The most probable is the following mechanism of their formation. In microplasma arc column at currents below 35 A, heating of the majority of particles of 63 to 160  $\mu\text{m}$  size to melting temperature  $T_{\text{melt}}$  is improbable [16]. Powder, including that with inner micropores, penetrates into weld pool in solid aggregate state ( $T_{\text{pore}} < T_{\text{melt}}$ ). Further heating and melting of disperse

particles in the weld pool requires considerable additional losses of thermal energy that causes violation of boundary condition of the third kind\*. Energy store that can be spent for powder heating and melting is characterized by the magnitude of thermal energy of pool molten metal overheating and time of its staying in the liquid aggregate state. Disperse filler feeding lowers weld pool average temperature, and its maximum admissible quantity is limited [16, 22]. Powder particle inside the molten metal volume can be regarded as «thermally thin body»\*\*. Time of its heating up to  $T_{\text{melt}}$  is directly proportional to its diameter and temperature difference  $T_{\text{melt}} - T_{\text{pore}}$ , and is inversely proportional to specific thermal energy falling to its surface [23].

Powder distribution at its addition to the weld pool follows a normal law [14], and time of pool metal existence in the molten state is limited [1]. Depending on the quantity of energy, obtained by each particle from overheated metal, five cases

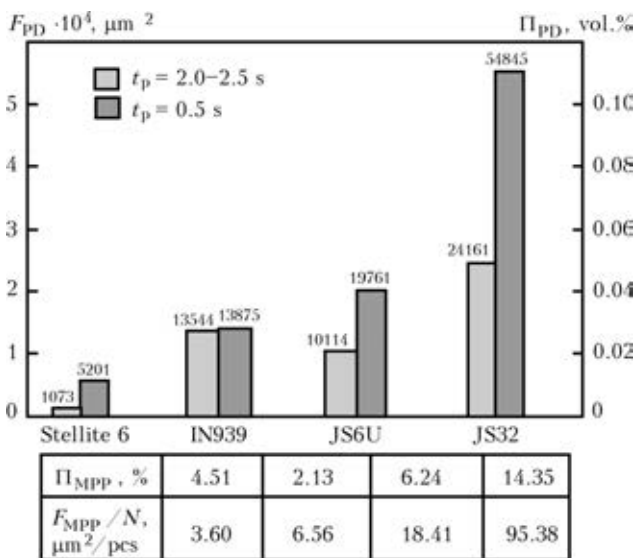


**Figure 7.** Influence of filler powder microporosity values on deposited metal microporosity characteristics for various alloys at  $I = 10-15$  A

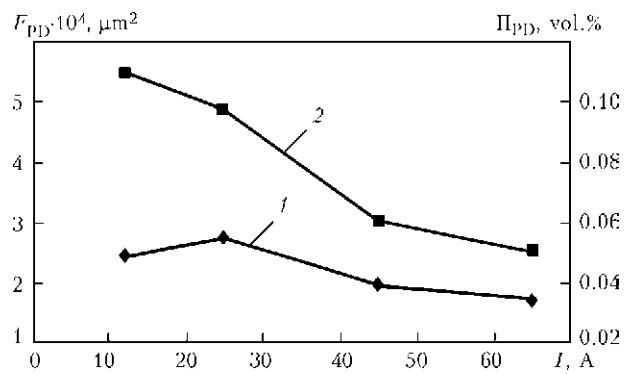


**Figure 8.** Influence of welding current on microporosity characteristics of JS32 deposited metal at different time periods between addition of powder microporions of weight  $M_0 = 0.12-0.14$  g to weld pool: 1 –  $t_p = 2.0-2.5$  s; 2 – 0.5 s (powder of JS32-VI alloy corresponds to III batch acc. to Table 1)

\*Amount of thermal energy, arriving to its surface as a result of convective and radiation heat extcpage, equal to the amount of energy removed through heat conductivity [23].

\*\*Bodies, in which temperature gradient arising in their section is negligibly small [23].

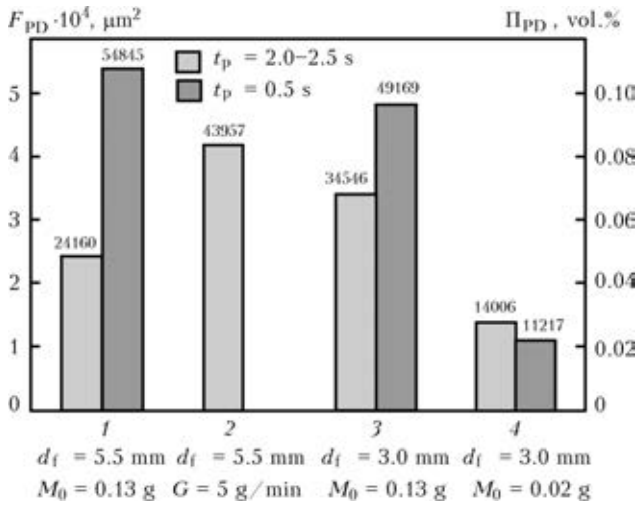


**Figure 9.** Influence of process parameters and kind of filler feed (1, 3, 4 – portioned; 2 – continuous) on microporosity characteristics of JS32 deposited metal at  $I = 10-15$  A (powder from JS32-VI alloy corresponds to III batch acc. to Table 1)

are possible at the moment of weld pool solidification (Figure 10). The last three of them lead to discontinuities in the deposited metal and then are visually observed at metallographic analysis (see Figure 5). At present it is not known, which process predominates at micropore formation in the deposited metal at the moment of its solidification in the weld pool:

- particle with inner micropore does not have enough time to heat up to  $T_{melt}$  and to melt;
- gas bubble released from inner discontinuity of filler particle does not have enough time to float to the surface and forms a micropore.

Porosity formation by the mechanism, different from the generally known one [1], is also

observed in laser welding of austenitic stainless steels [24].

Proceeding from the established interrelation between microporosity in filler powder and in deposited metal, the following goals are urgent:

- development of simple and reliable methods of quantitative control of inner discontinuities in filler powders for microplasma powder surfacing;
- optimization of melt dispersion technology in production of nickel alloy powders with more than 45 vol.% of  $\gamma'$ -phase.

The following procedures can be promising for disperse filler control: metallographic analysis of powder particle cross-sections determining the area, quantity and parameters of statistical distribution of micropores depending on particle size, and evaluation of picnometric density and porosity of powder by hydrostatic weighing.

Preliminary evaluation of picnometric density of JS32-VI alloy powder showed that for disperse filler with a smaller quantity of porous particles its average value differs by not more than 4.6 % from alloy material density (Table 2).

Proceeding from the known features of nickel superalloy metallurgy in vacuum-induction melting [17, 19], increased content of oxygen and nitrogen in the initial billet or charge can have an additional influence of susceptibility to micropore formation in manufacture of the respective powders. First, during molten metal dispersion running of the reaction of interaction of oxygen with carbon (up to 0.15–0.18 wt.% content) with precipitation of gaseous oxide or dioxide is probable [17]. Secondly, at increased nitrogen content of 0.0024–0.0050 wt.% susceptibility of

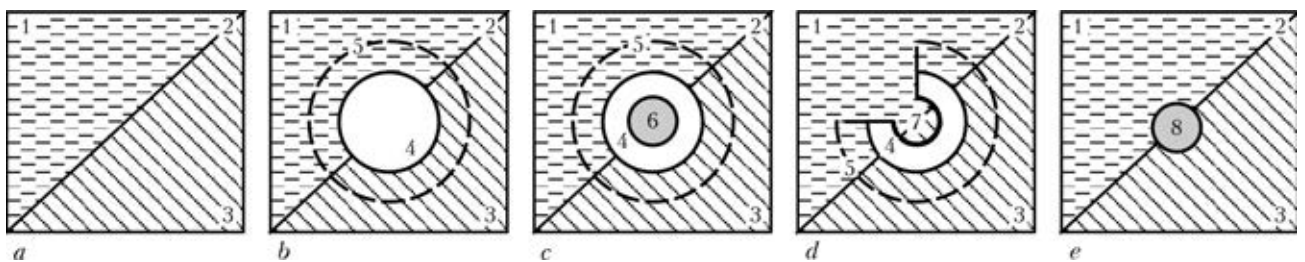


**Figure 10.** Schematics of possible states of powder particles at the moment of weld pool solidification: a, e – totally melted; b – unmolten particle without micropore; c, d – unmolten particle with micropore; 1 – molten metal; 2 – solidification front; 3 – solidified metal; 4 – powder particle; 5 – possible area of molten metal local overcooling and further local solidification from particle surface; 6 – closed micropore in particle; 7 – open micropore in particle; 8 – gas bubble released from molten particle with closed micropore

**Table 2.** Microporosity characteristics of filler powder from JS32-VI alloy (by hydrostatic weighing data)

Parameter	I batch	II batch	III batch
Powder picnometric density $\rho_p$ , g/cm <sup>3</sup>	8.489 <sup>+0.1435</sup> <sub>-0.1629</sub>	8.3381 <sup>+0.1285</sup> <sub>-0.1394</sub>	8.1547 <sup>+0.4645</sup> <sub>-0.3162</sub>
Porosity $\rho$ , %	3.097 <sup>-1.3974</sup> <sub>+2.0037</sub>	4.5881 <sup>-1.5910</sup> <sub>+1.4677</sub>	6.9098 <sup>-5.3025</sup> <sub>+3.6097</sub>
Alloy density $\Pi_{wt}$ acc. to [25], $\rho$ , g/cm <sup>3</sup>	8.76		
Alloy density $\rho$ , g/cm <sup>3</sup> (weighing of 75 × 45 × 3.5 mm ground plate)	8.79		



cast nickel alloys with single-crystal structure to microporosity formation is manifested [19].

### Conclusions

1. Sound formation of deposited metal in microplasma powder surfacing on narrow substrate from nickel superalloys is ensured by limiting oxygen to less than 0.018 and of nitrogen to 0.0055 wt.% in it.

2. It is shown that active gas content in nickel superalloy gradually increases, as it goes through the cast billet or charge—disperse powder—deposited metal technological stages. It is necessary to control and limit their content after the first two processing stages so that the quantity of oxygen and nitrogen in the deposited metal did not exceed 0.018 and 0.0055 wt.%, respectively.

3. In filler powders for microplasma powder surfacing it is rational to have not more than 0.012 wt.% O and not more than 0.0025 wt.% N. At up to 0.002 wt.% gas content in the initial billet or charge, this is achieved by ingot dispersion by argon.

4. Formation of micropores of 5 to 75  $\mu\text{m}$  size in the deposited metal is associated with presence of inner micropores of similar size in filler powder. It is established that microporosity in deposited metal depends on micropore content in initial powder, welding current, filler microporosity weight, concentration and frequency of its addition to the weld pool. Minimum level of microporosity in deposited metal JS32 (0.02–0.03 vol.% in bead longitudinal section) is observed at lowering of fed filler powder microporosity weight to 0.02 g.

5. The most probable is micropore transfer with disperse filler into weld pool through microplasma arc. In the pool at the moment of its metal solidification the particle with micropore either does not have enough time to melt, or after its melting the gas bubble does not have enough time to float to pool surface.

6. In-coming inspection of batches of nickel superalloy powders for micropore content in their particles is required. Promising control procedures are evaluation of picnometric density of disperse material and statistic metallographic analysis. It is established that the average picnometric density of filler powders with smaller micropore content deviates from alloy material density by not more than 4.6 %.

1. (1974) *Technology of electric fusion welding of metals and alloys*. Ed. by B.E. Paton. Moscow: Mashinostroenie.

2. Sims, C., Stoloff, N., Hagel, W. (1995) *Superalloys II: Heat-resistant materials for aerospace and industrial power plants*. Ed. by R.E. Shalin. Moscow: Metallurgiya.
3. Zinke, M., Neubert, G., Herold, H. (1999) Properties of welded joints of heat-resistant nickel-base alloys. *Avtomatich. Svarka*, **4**, 35–38.
4. Sorokin, L.I. (2004) Welding-up of cracks with oxidized surface on heat-resistant nickel alloys. *Svarochn. Proizvodstvo*, **12**, 30–31.
5. Sorokin, L.I., Lukin, V.I., Bagdasarov, Yu.S. (1997) Weldability of cast heat-resistant alloys of JS6 type. *Ibid.*, **6**, 12–17.
6. Sorokin, L.I. (1999) Strains and cracks in welding and heat treatment of heat-resistant nickel alloys. *Ibid.*, **12**, 11–17.
7. Yushchenko, K.A., Savchenko, V.S., Yarovitsyn, A.V. et al. (2010) Development of the technology for repair by microplasma powder cladding of flange platform faces of aircraft engine D18T high-pressure turbine blades. *The Paton Welding J.*, **8**, 21–24.
8. (2010) Deloro Stellite technological seminar in Zaporozhie. *Ibid.*, **1**, 59–62.
9. Yushchenko, K.A., Yarovitsyn, A.V., Zvyagintseva, A.V. (2008) Properties of microplasma powder welded joints on heat-resistant nickel alloys. *Ibid.*, **9**, 2–5.
10. Ternovoj, Yu.F., Kudievsky, S.S., Pashetneva, N.N. (2005) *Engineering calculations of melted metal spraying processes*. Zaporozhie: Zaporozh. GIA.
11. Ternovoj, Yu.F., Baglyuk, S.A., Kudievsky, S.S. (2008) *Theoretical principles of metallic melt spraying*. Zaporozhie: Zaporozh. GIA.
12. Fedorenko, G.A., Shvedikov, V.M., Grishchenko, L.V. (1986) About reliability of methods for examination of jet shielding. *Svarochn. Proizvodstvo*, **6**, 35–37.
13. *GOST 17745–90: Steels and alloys. Methods for determination of gases*. Introd. 01.07.1991.
14. Yushchenko, K.A., Yarovitsyn, A.V., Yakovchuk, D.B. et al. (2013) Some techniques for reducing filler powder losses in microplasma cladding. *The Paton Welding J.*, **9**, 30–36.
15. Bulanov, V.Ya., Kvater, L.I., Dolgal, T.V. et al. (1983) *Diagnostics of metallic powders*. Moscow: Nauka.
16. Gladky, P.V., Pereplyotchkov, E.F., Ryabtsev, I.A. (2007) *Plasma surfacing*. Kiev: Ekotekhnologiya.
17. Kablov, E.N. (2001) *Cast blades of gas turbine engines (alloys, technology, coatings)*. Moscow: MISIS.
18. Stroganov, G.B., Chepkin, V.M. (2000) *Cast heat-resistant alloys for gas turbines*. Moscow: ONTI MATI.
19. Kablov, D.E., Sidorov, V.V. (2012) Nitrogen in monocrystalline heat-resistant alloys. *Nauka i Obrazovanie*, **2**, 77-30569/339556 (electron. ed.).
20. Lysenko, N.A., Pedash, A.A., Kolomojtsjev, A.G. et al. (2005) Improvement of structure and properties of nickel heat-resistant alloy ZM13U-VI. *Visnyk Zaporizh. DTU*, **2**, 34–39.
21. Yarovitsyn, A.V., Yushchenko, K.A., Nakonechny, A.A. et al. (2009) Peculiarities of low-amperage argon-arc and microplasma powder cladding on narrow substrate. *The Paton Welding J.*, **6**, 31–35.
22. Ivochkin, I.I., Malyshev, B.D. (1981) *Submerged-arc welding with additional filler metal*. Moscow: Strojizdat.
23. Lykov, A.V. (1967) *Theory of heat conductivity*. Moscow: Vysshaya Shkola.
24. Katayama, S. (2001) Mechanism of formation of different defects in laser welding and methods of their prevention. *J. JWS*, **19**(1), 213–218.
25. Sharova, N.A., Tikhomirova, E.A., Barabash, A.L. et al. (2009) To problem of choice of new heat-resistant nickel alloys for prospective aircraft gas-turbine engines. *Vestnik Samara GAU*, **3**, 249–255.

Received 30.04.2014